



PERGAMON

Chemosphere: Global Change Science 1 (1999) 83–90

CHEMOSPHERE—  
GLOBAL CHANGE  
SCIENCE

## Is the biomass burning source of CO decreasing?

Y.L. Yung<sup>a,\*</sup>, C. Shia<sup>a</sup>, R.L. Herman<sup>b</sup>

<sup>a</sup> Division of Geological and Planetary Science, California Institute of Technology, Pasadena, CA 91125, USA

<sup>b</sup> Jet Propulsion Laboratory, California Institute of Technology, Pasadena, CA 91109, USA

Received 16 April 1998; accepted 15 December 1998

*Importance of this Paper: This paper is a preliminary analysis of CO and methane mixing ratios measured by NOAA–CMDL global cooperative flask sampling network. From the seasonality of recent trends in these gases, we infer that most of the observed decrease in tropospheric CO during the early 1990s can be attributed to a decrease in biomass burning.*

### Abstract

To investigate secular changes in CO and CH<sub>4</sub>, we examined monthly means of tropospheric measurements made from samples collected at 19 fixed sites in the National Oceanic and Atmospheric Administration (NOAA) Climate Monitoring and Diagnostics Laboratory (CMDL) global cooperative flask sampling network. The CH<sub>4</sub> data are available for the period 1984–1995. A somewhat shorter time series is available for CO (1989–1995). The data were analyzed to extract a consistent pattern of change in time and in latitude. The most important preliminary finding is that the patterns of CO and CH<sub>4</sub> change appear to resemble that of biomass burning. That is, there is maximum change during local spring in both northern and southern hemispheres. If we attribute a significant part of the change in CH<sub>4</sub> trend (3–6 ppb/yr) to biomass burning, the corresponding change in CO is approximately 2–5 ppb/yr. This would explain the bulk of the observed change in CO (4–7 ppb/yr). © 1999 Elsevier Science Ltd. All rights reserved.

*Keywords:* Carbon monoxide; Methane; Trend; Biomass burning

### 1. Introduction

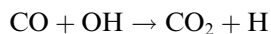
One of the most important roles of the earth's troposphere is its oxidative capacity, the ability to oxidize a large number of chemical species, thereby removing them from the atmosphere. The species that are oxidized in the troposphere include CH<sub>4</sub>,

CH<sub>3</sub>Cl, CH<sub>3</sub>Br, CO, substituted chlorofluorocarbons (e.g., CHClF<sub>2</sub> (HCFC-22)), non-methane hydrocarbons (e.g., C<sub>2</sub>H<sub>6</sub>) and oxides of nitrogen. Any change in the oxidative capacity of the atmosphere would result in a change in the lifetimes of the above mentioned species which are important in regulating the ozone layer and/or are important greenhouse molecules (e.g. Thompson, 1992).

The oxidative capacity of the troposphere is strongly influenced by CO and CH<sub>4</sub> (e.g. Crutzen,

\* Corresponding author. Tel.: +1-626-395-6940; e-mail: yly@gps.caltech.edu

1995). Although the primary oxidant, OH, is produced by the reaction of H<sub>2</sub>O with O(<sup>1</sup>D) (Levy, 1972; Logan et al., 1981; Crutzen and Zimmermann, 1991), CO and CH<sub>4</sub> play fundamental roles in the chemistry of OH because of the two key reactions:



The former reaction recycles OH to HO<sub>2</sub>, another member of the odd hydrogen family (HO<sub>x</sub>), and plays a crucial role in determining the partitioning of HO<sub>x</sub>. The latter reaction is ultimately a net source of CO and HO<sub>x</sub> (e.g. Logan et al., 1981; Crutzen, 1995). Indeed, OH, CO, and CH<sub>4</sub> form a strongly coupled system such that the response to any perturbation is non-linear and may take a much longer time to recover than that of a decoupled system (Sze, 1977; Prather, 1994). CO is also important to atmospheric chemistry by playing a role in tropospheric O<sub>3</sub> production and destruction (e.g. Fishman and Crutzen, 1978; Seiler and Fishman, 1981; Crutzen, 1995). In low NO<sub>x</sub> environments, CO oxidation leads to O<sub>3</sub> destruction. O<sub>3</sub> reacts with HO<sub>2</sub> to create OH, but the CO oxidation reaction shown above recycles HO<sub>2</sub>. However, in high NO<sub>x</sub> environments, oxidation of CO, CH<sub>4</sub>, or non-methane hydrocarbons leads to O<sub>3</sub> production (e.g. Crutzen, 1995). HO<sub>2</sub> reacts rapidly with NO instead of O<sub>3</sub>. Both HO<sub>2</sub> and RO<sub>2</sub> convert NO to NO<sub>2</sub>, and subsequent photolysis of NO<sub>2</sub> leads to production of O<sub>3</sub>. According to Crutzen (1995) the globally averaged vertically integrated rate for the destruction of CO by OH and that for the destruction of CH<sub>4</sub> by OH are  $3.5 \times 10^{11}$  and  $10^{11}$  molecules cm<sup>-2</sup> s<sup>-1</sup>, respectively. These values are greater than the rate at which ozone is transported from the stratosphere,  $4 \times 10^{10}$  molecules cm<sup>-2</sup> s<sup>-1</sup>. Thus the sources and sinks of tropospheric ozone are dominated by photochemistry that requires the presence of CO or hydrocarbons.

A recent overview of the composition of the troposphere described decreases in the trends of CO and CH<sub>4</sub> (Khalil and Rasmussen, 1995). Recent measurements (from 1979 to 1994) presented there indicate that CO mixing ratios in the atmo-

sphere decreased by approximately 4–7 parts per billion per year (ppb/yr) over that time period. At the same time, the growth trend of CH<sub>4</sub> has decreased from about 12 ppb/yr in 1984–1988 to roughly 6 ppb/yr a decade later. These changes are of considerable importance to the oxidative capacity of our global atmosphere. The key questions are what drives these changes and whether the changes in CO and CH<sub>4</sub> are related to a common cause?

To investigate changes in CO and CH<sub>4</sub>, we examined monthly means of tropospheric measurements made from samples collected at six of the nineteen fixed sites in the National Oceanic and Atmospheric Administration (NOAA) Climate Monitoring and Diagnostics Laboratory (CMDL) global cooperative flask sampling network (Dlugokencky et al., 1996). The CH<sub>4</sub> data are available for the period 1984–1995. A somewhat shorter time series is available for CO (1989–1995). The data were analyzed to extract a consistent pattern of change in time and in latitude.

## 2. Data analysis

We shall first illustrate our method of analysis using the NOAA–CMDL measurements of CO and CH<sub>4</sub> from the Mauna Loa Observatory (19.5 N, 155.5 W), Hawaii, hereafter referred to as MLO. Although our primary goal is to understand the trend in CO, we shall use the CH<sub>4</sub> data as additional support for our conclusion because of the longer time record of CH<sub>4</sub>. It is reasonable to expect that CH<sub>4</sub> and CO abundances are related because CH<sub>4</sub> oxidation provides a major source of CO (e.g. Logan et al., 1981), and because the biomass burning sources of CO and CH<sub>4</sub> appear to be proportional (e.g. Andreae et al., 1996; Blake et al., 1996). At the end of this section, we will examine CO and CH<sub>4</sub> data from other oceanic NOAA–CMDL stations.

### 2.1. Carbon monoxide

Fig. 1(a) shows the monthly mean NOAA–CMDL measurements of CO (ppb) at MLO from 1990 to 1995. The data from four other stations

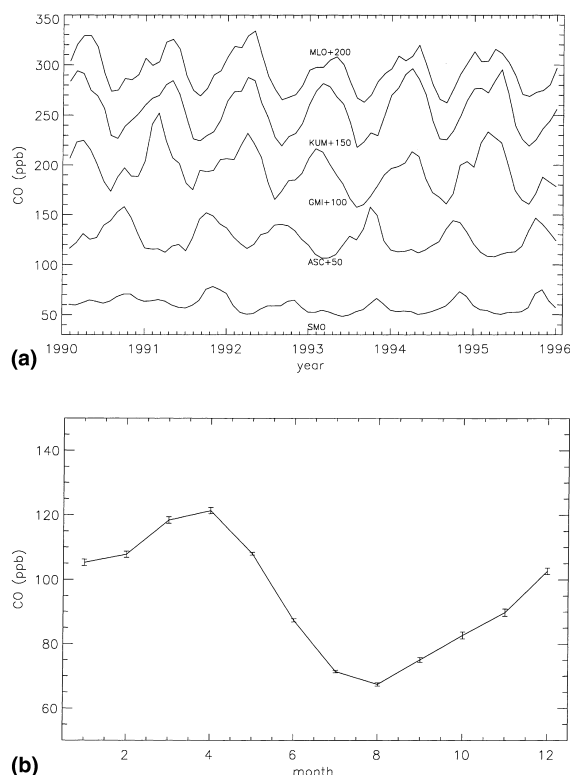


Fig. 1. (a) Monthly mean CO mixing ratios (ppb) at Mauna Loa Observatory (MLO), Hawaii (19.5 N, 155.5 W) and four other remote sites listed in Table 1. Data were obtained by the NOAA–CMDL global cooperative flask sampling network. (b) Mean seasonal cycle of CO (ppb) at MLO derived from the average of the data from 1990 to 1995 (shown in Fig. 1(a)). Error bars represent  $\pm 1$  standard deviation.

(chosen to be remote sites) are shown for comparison (see Table 1 for the locations of the stations). The most prominent feature of this figure is the large seasonal cycle with maximum CO in late winter to early spring and minimum CO in sum-

mer. Fig. 1(b) shows the seasonal cycle of CO at MLO, obtained from the arithmetic mean of six years of data in Fig. 1(a). The error bars are standard deviations based on the six-year dataset. Minimum CO mixing ratios in summer are determined by a balance between CO loss via the CO + OH reaction and CO production from oxidation of CH<sub>4</sub> and non-methane hydrocarbons (e.g. Logan et al., 1981). The concentrations of OH are greatest in the summer because of enhanced solar insolation and more water vapor in the atmosphere.

In order to obtain a monthly-dependent trend at MLO, we separate the CO data by month and fit a least-squares linear regression through the six-year time series for each month. Representative monthly trends for the months of March, June, September, and December are shown in Figs. 2(a)–(d). The slopes of the linear fits to these monthly trends are shown in Fig. 3. The mean slope is  $-2$  ppb/yr. However, the slopes of the monthly trends are significantly steeper in spring, with values of approximately  $-4$  ppb/yr. Monthly trends are much smaller in the other seasons. We will show next that this pattern of change is consistent with that deduced for trends in CH<sub>4</sub> mixing ratios.

## 2.2. Methane

Fig. 4 shows monthly mean NOAA–CMDL measurements of CH<sub>4</sub> (ppb) at MLO, South Pole Station (SPO) and four other remote sites (see Table 1 for location of sites) for the years 1984–1995. The most prominent features in this figure are the long-term growth trend of CH<sub>4</sub> and the seasonal cycle, but the most interesting aspect of these data is the change in the growth trend. There

Table 1  
NOAA–CMDL stations used in the CO and CH<sub>4</sub> data analysis

Station	Full name	Lat., Lon.	Years for CO data	Years for CH <sub>4</sub> data
MLO	Mauna Loa	19.5 N, 155.5 W	1990–95	1984–95
KUM	Cape Kumukahi	19.5 N, 155.8 W	1990–95	1984–95
GMI	Guam	13.4 N, 144.8 W	1990–95	1984–95
ASC	Ascension	7.6 S, 14.2 W	1990–95	1984–95
SMO	American Samoa	14.2 S, 170.3 W	1989–95	1984–95
SPO	South Pole	90.0 S, 24.8 W	Not used	1984–95

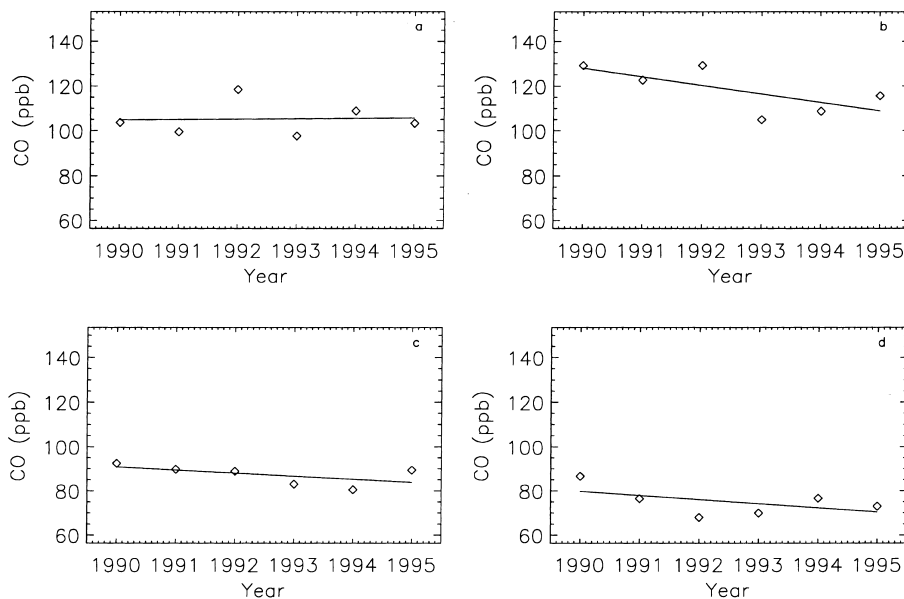


Fig. 2. Monthly trends of monthly mean CO mixing ratios (ppb) at MLO for the months of March (a), June (b), September (c) and December (d). Solid lines are least-squares linear regressions to the monthly mean data.

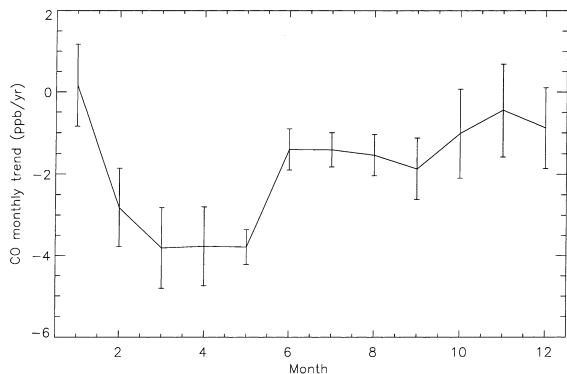


Fig. 3. Slopes of CO monthly trends (ppb/yr) at MLO, derived from CO measurements from 1990 to 1995, using the method described in the text. Error bars represent  $\pm 1$  standard deviation.

is a noticeable change in the slope of the data in the later period as compared with that in the earlier years (e.g. Khalil and Rasmussen, 1995; Dlugokencky et al., 1996).

First, we analyze the  $\text{CH}_4$  data from MLO. For convenience, we divide the 12 yr of data into three overlapping six-year periods: (a) 1984–1989, (b) 1987–1992, and (c) 1990–1995. Applying the same

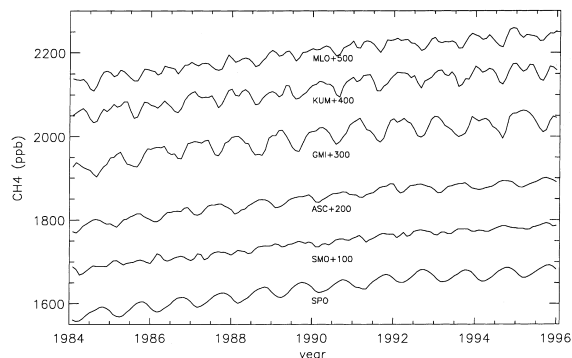


Fig. 4. Monthly mean  $\text{CH}_4$  mixing ratios (ppb) measured by the NOAA–CMDL flask sampling network for the six stations listed in Table 1.

technique as we have done with the CO data, we obtain the monthly trends for the three periods, as shown in Fig. 5. The earlier period (a) has a much larger trend (about 12 ppb/yr) than the later period (c) (about 6 ppb/yr). However, the seasonal pattern of the trend has also changed, as can be seen by taking the differences between the monthly trends of each period (Fig. 6). The difference be-

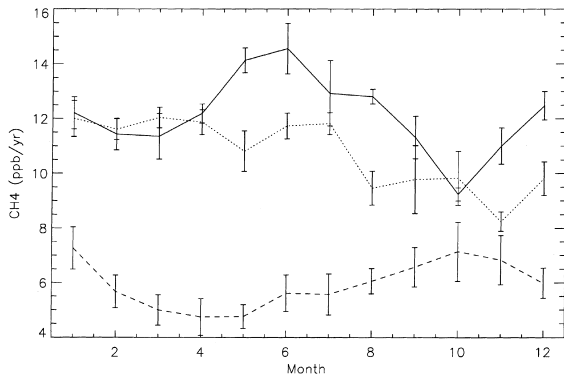


Fig. 5. Monthly trends in  $\text{CH}_4$  (ppb/yr) at MLO. Solid line: period (a) from 1984 to 1989; Dotted line: period (b) from 1987 to 1992; Dashed line: period (c) from 1990 to 1995. Error bars represent  $\pm 1$  standard deviation.

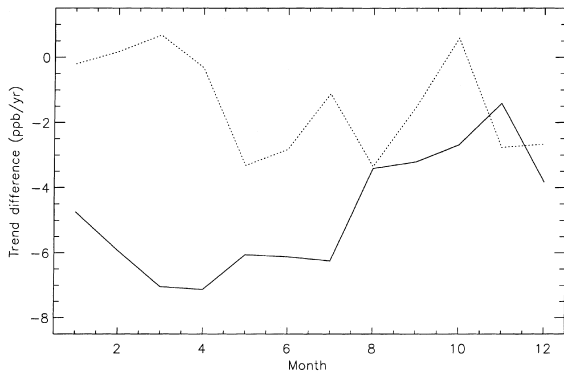


Fig. 6. Difference in  $\text{CH}_4$  trends between periods (ppb/yr) at MLO. Dotted line: difference between periods (b) and (a); Solid line: difference between periods (c) and (b).

tween periods (b) and (a) (dotted line) does not show a clear seasonal dependence. However, the difference between periods (c) and (b) (solid line) shows a pronounced change in spring that resembles the springtime  $\text{CO}$  monthly trends (Fig. 3).

The change in  $\text{CH}_4$  trends at SPO stands in contrast to that at MLO. Applying the same analysis to the SPO data, the  $\text{CH}_4$  monthly trends for the periods (a), (b), and (c) are presented in Fig. 7. Compared to Fig. 5, there is much less seasonal variation in these data. The differences in trends between periods (b) and (a) (dotted line) and between periods (c) and (b) (solid line) are shown in Fig. 8. Again, the SPO data show much

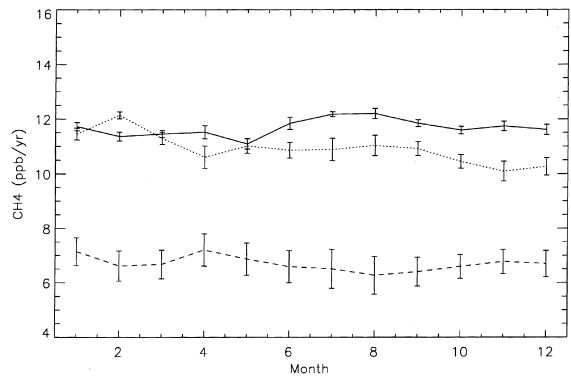


Fig. 7. Monthly trends in  $\text{CH}_4$  (ppb/yr) at SPO. Solid line: period (a) from 1984 to 1989; Dotted line: period (b) from 1987 to 1992; Dashed line: period (c) from 1990 to 1995. Error bars represent  $\pm 1$  standard deviation.

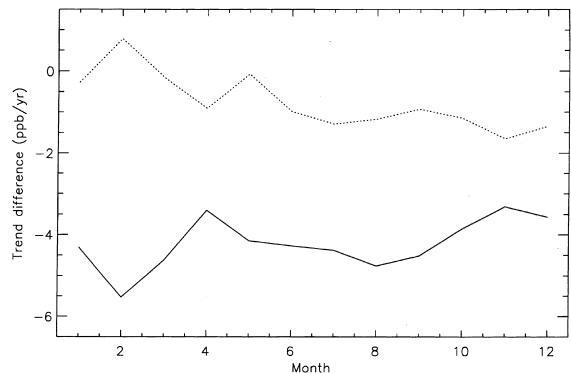


Fig. 8. Difference in  $\text{CH}_4$  trends between periods (ppb/yr) at SPO. Dotted line: difference between periods (b) and (a); Solid line: difference between periods (c) and (b).

less seasonal variation than the MLO data in Fig. 6. The reason is that SPO is an extremely remote site, so the  $\text{CH}_4$  that reaches there has been averaged over months in transit. The small level of variation in this difference between derivatives of SPO data, more than anything else, demonstrates the high precision of the NOAA–CMDL measurements.

### 2.3. Spatial and seasonal patterns of change

In order to derive a spatial and seasonal pattern of change for  $\text{CO}$ , we selected five NOAA–CMDL stations: MLO, KUM, GMI, ASC, and SMO. The

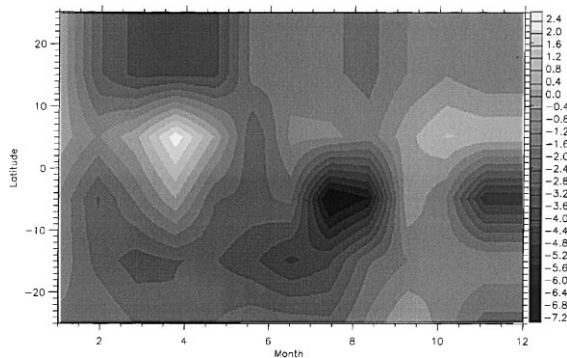


Fig. 9. Contour plot of monthly trends in CO (ppb/yr) for each month from 25 S to 25 N. The data used in this plot are from NOAA–CMDL stations SMO, ASC, GMI, KUM, and MLO.

station locations and time periods of available CO data are summarized in Table 1. These stations have been chosen because they are oceanic sites unlikely to be contaminated by continental or local sources of CO. The signal we wish to extract is so small that it will be completely masked by local fluctuations. We also need a sufficient number of years of data to have confidence in the monthly trends. The method of extracting a monthly trend for each data set is the same as described earlier for CH<sub>4</sub>. Monthly trends of CO from these five stations are shown in Fig. 9.

The CO monthly trends are generally negative (0 to  $-7$  ppb/yr) over the time period 1990–1995, except at Ascension Island (ASC), which may be influenced by continental sources of CO. There appears to be a strong seasonal dependence in the monthly trends. This may be compared with the spatial and temporal pattern of biomass burning, as shown in Fig. 10 on the basis of data compiled by Hao and Liu (1994). Some cautionary statements would be in order. The model of Hao and Liu tends to have too much burning late in the dry period and too little in the early part of the dry season (M.O. Andreae, pers. comm.). Thus the spatial and temporal pattern of biomass mass burning shown in Fig. 10 is suggestive rather than definitive.

To provide additional evidence for the relation between CO change and biomass burning, we analyzed CH<sub>4</sub> data from six CMDL stations: MLO,

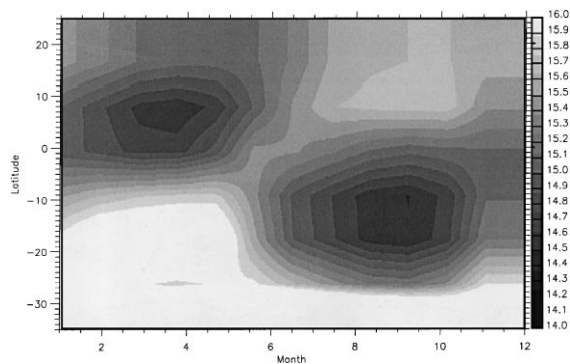


Fig. 10. Contour plot of the rate,  $R$ , of biomass burning (g C/yr) in each month from 35 S to 25 N, based on Hao and Liu (1994). The contours are  $\log_{10}(R)$ .

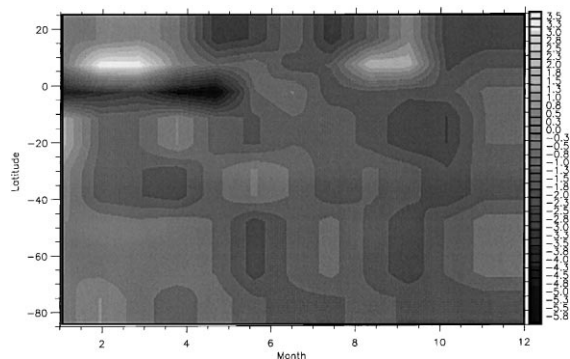


Fig. 11. Contour plot of the difference in CH<sub>4</sub> trends in each month (ppb/yr) between periods (b) and (a) from 85 S to 25 N. Data used in this plot are from NOAA–CMDL stations SMO, ASC, GMI, KUM, MLO, and SPO.

KUM, GMI, ASC, SMO, and SPO. Station locations and time periods of available data are summarized in Table 1. Following the method described earlier, we divided the 12 yr of data from 1984 to 1995 into three periods: (a), (b), and (c). The trends for each six-year period were computed as before. The difference in trends (ppb/yr) between periods (b) and (a) is shown in Fig. 11. Aside from a large negative trend in the tropics during the early part of the year, there seems to be no simple consistent pattern to the difference between periods (b) and (a). In contrast, the difference in trends between periods (c) and (b) (Fig. 12) shows maximum changes during local spring in

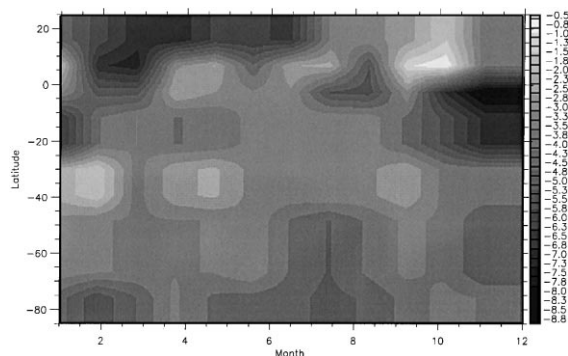


Fig. 12. Same as Fig. 11 (ppb/yr), between periods (c) and (b).

both northern and southern hemispheres. This pattern of change is similar to the pattern of biomass burning (Fig. 10). We therefore conclude that the most likely explanation for the change in  $\text{CH}_4$  trends in the period 1984–1995 is a change in the rate of biomass burning.

### 3. Discussion

The temporal pattern of change for both CO and  $\text{CH}_4$  at MLO suggests that there has been a decreasing source during spring in the northern hemisphere. A similar analysis carried out for data from several NOAA–CMDL stations suggests that there has been a similar decreasing source during spring in the southern hemisphere. This pattern of change is consistent with a decrease in biomass burning, which peaks in the spring season of each hemisphere (Hao and Liu, 1994). If we attribute a significant part of the declining upward trend in  $\text{CH}_4$  (3–6 ppb/yr) to biomass burning, we can estimate the corresponding change in CO using the empirically determined ratio of 0.1 (v/v) for  $\text{CH}_4/\text{CO}$  release in biomass burning (Blake et al., 1996). The inferred decline in the trend for CO is 2–5 ppb/yr. This would explain the bulk of the observed change of 4–7 ppb/yr in the CO trend. The remainder of the observed change could be due to a combination of factors, including changes in column  $\text{O}_3$  or tropospheric temperatures (Granier et al., 1996). Our results are consistent with earlier suggestions of changes in the biomass

burning source of CO on the basis of  $^{13}\text{C}$  data (Lowe et al., 1994, 1997) and a recent three-dimensional modeling study (Granier et al., 1996), but this appears to be the first attempt to extract information from the observed seasonal pattern. In the future, this analysis will be expanded by using CO measurements from more oceanic stations over a longer time period. In this way, we hope to gain a better understanding of the impact of biomass burning on the global atmosphere, particularly its impact on  $\text{O}_3$  (e.g. Jiang and Yung, 1996).

### Acknowledgements

We thank J.P. Pinto, J. Wang, M.O. Andreae, E.J. Moyer, and two anonymous reviewers for helpful comments, and E.J. Dlugokencky and P.C. Novelli of NOAA–CMDL for the use of  $\text{CH}_4$  and CO data from the NOAA–CMDL global flask sampling network. Supported by NASA grant NAG1-1806 to the California Institute of Technology. Contribution 5765 from the Division of Geological and Planetary Sciences, California Institute of Technology.

### References

- Andreae, M.O., et al. 1996. Trace gas and aerosol emissions from savanna fires. In: Levine, J.S. (Ed.), *Biomass Burning and Global Change*. MIT Press, Cambridge, MA, pp. 278–295.
- Blake, N.J., et al. 1996. In: Levine, J.S. (Ed.), *Biomass Burning and Global Change*. MIT Press, Cambridge, MA.
- Crutzen, P.J., 1995. Ozone in the troposphere. In: Singh, H.W. (Ed.), *Composition, Chemistry, and Climate of the Atmosphere*. Van Nostrand Reinhold, New York, chapter 10, pp. 50–87.
- Crutzen, P.J., Zimmermann, P.H., 1991. The changing photochemistry of the troposphere. *Tellus* 43, 136–151.
- Dlugokencky, E.J., Dutton, E.G., Novelli, P.C., Tans, P.P., Masarie, K.A., Lantz, K.O., Madronich, S., 1996. Changes in  $\text{CH}_4$  and CO growth rates after the eruption of Mt. Pinatubo and their link with changes in tropical tropospheric UV flux. *Geophys. Res. Lett.* 23, 2761–2764.
- Fishman, J., Crutzen, P.J., 1978. The origin of ozone in the troposphere. *Nature* 247, 855–858.
- Granier, C., Muller, J-F., Madronich, S., Brasseur, G., 1996. Possible causes for the 1990–1993 decrease in the global

- tropospheric CO abundances: A three-dimensional sensitivity study. *Atmos. Env.* 30, 1673–1682.
- Hao, W.M., Liu, M.H., 1994. Spatial and temporal distribution of tropical biomass burning. *Global Biogeochemical Cycles* 8, 495–503.
- Jiang, Y., Yung, Y.L., 1996. Concentrations of Tropospheric Ozone from 1979 to 1992 over tropical Pacific South America from TOMS data. *Science* 272, 714–716.
- Khalil, M.A.K., Rasmussen, R.A., 1995. The changing composition of the earth's atmosphere. In: Singh, H.W. (Ed.), *Composition, Chemistry, and Climate of the Atmosphere*. Van Nostrand Reinhold, New York, chapter 3, pp. 50–87.
- Levy II, H., 1972. Photochemistry of the lower troposphere. *Planet. Space Sci.* 20, 919–935.
- Logan, J.A., Prather, M.J., Wofsy, S.C., McElroy, M.B., 1981. Tropospheric chemistry: A global perspective. *J. Geophys. Res.* 86, 7210–7254.
- Lowe, D.C., Brenninkmeijer, C.A.M., Brailsford, G.W., Lasey, K.R., Gomez, A.J., 1994. Concentrations and  $^{13}\text{C}$  records of atmospheric methane in New Zealand and Antarctica: Evidence for changes in methane sources. *J. Geophys. Res.* 99, 16913–16925.
- Lowe, D.C., Manning, M.R., Brailsford, G.W., Bromley, A.M., 1997. The 1991–1992 atmospheric methane anomaly – southern-hemisphere  $^{13}\text{C}$  decrease and growth-rate fluctuations. *Geophys. Res. Lett.* 24 (8), 857–860.
- Prather, M.J., 1994. Lifetimes and eigenstates in atmospheric chemistry. *Geophys. Res. Lett.* 21, 801–804.
- Seiler, W., Fishman, J., 1981. The distribution of carbon monoxide and ozone in the free troposphere. *J. Geophys. Res.* 86, 7255–7265.
- Sze, N.D., 1977. Anthropogenic CO emissions: implications for the atmospheric CO–OH–CH<sub>4</sub> cycle. *Science* 256, 1157–1165.
- Thompson, A.M., 1992. The oxidizing capacity of the earth's atmosphere: Probable past and future changes. *Science* 256, 1157–1165.

**Dr. Yuk Ling Yung**, is a Professor of Planetary Science at the Division of Geological and Planetary Sciences, California Institute of Technology. He received his Ph.D. degree in Physics at Harvard University. He came to Caltech as an assistant professor to build up a modeling group specializing in the chemical composition of earth and planetary atmospheres. His modeling interests include radiation, dynamics, chemistry, planetary evolution and biosphere. He is the author of two books and more than 100 professional papers. Dr. Yung was a member of the Voyager ultraviolet experiment and is a co-investigator on the Galileo photopolarimeter experiment and the Cassini orbiter ultraviolet spectrometer investigation.